Journal of Advanced Research in Fluid Mechanics and Thermal Sciences

Journal homepage:
https://semarakilmu.com.my/journals/index.php/fluid_mechanics_thermal_sciences/index
ISSN: 2289-7879

Numerical Simulation of Boundary Layer Flow Over a Moving Plate in The Presence of Magnetic Field and Slip Conditions

Purnima Rai[1,*], Upendra Mishra[1]

[1] Department of Mathematics, Amity University Rajasthan, Kant, Kalwar, Jaipur, 303002, Rajasthan, India

ARTICLE INFO

Article history:
Received 9 February 2022
Received in revised form 25 April 2022
Accepted 28 April 2022
Available online 29 May 2022

Keywords:
Nanofluids; slip conditions; MHD; viscous dissipation; moving plate

ABSTRACT

This study demonstrates the viscous flow of nanofluids under the influence of magnetic field and slip conditions over the boundary layer in a moving plate. By applying appropriate similarity variables to the governing partial differential equations, a similarity transformation is implemented to obtain the same as non-linear ordinary differential equations. The Transformed equations are then numerically solved by the finite difference method. Various parameters such as plate velocity parameter, slip parameters, thermophoresis parameter and Brownian motion parameter, Eckert number, Prandtl number and Lewis number are examined to study the properties of flow and heat transfer. The coefficient of skin friction, Nusselt number, and Sherwood numbers for selected parameters are numerically presented. Impact of MHD, slip conditions and viscous dissipation on nanofluid temperature, concentration and velocity profiles are determined and analyzed via graphs. This research reveals that the presence of magnetic field and viscous dissipation contributes to increase in temperature profile. Moreover, it is found that, when velocity slip increases, the temperature profile increases while the velocity profile decreases. It thickens the concentration boundary layer as well. This work may find its significant applications in high temperature and cooling processes, space technology, paints, medicines, conductive coatings, cosmetics and bio-sensors.

1. Introduction

Convention Boundary layer flow is used extensively in engineering and industry. The subject of heat transmission in boundary layers has gained substantial attention in various studies for its extensive applications in industrial processes. Previously, low thermal conductivity cooling liquids including water, ethylene glycol, and oil were employed as pure fluids in many applications, but Choi and Eastman [8] introduced a new type of fluids termed nanofluids to overcome these restrictions in heat transfer enhancement in 1995. Nanofluids offer better thermophysical properties than base fluids like water. The properties and behaviour of nanofluids have been studied by various researchers. Buongiorno [6] established a nanofluid model in which thermophoresis and Brownian motion were considered to be two major slip mechanisms. Further, Kuznetsov and Nield [18] used

* *Corresponding author.*
E-mail address: purnima.rai411@gmail.com

https://doi.org/10.37934/arfmts.95.2.120136

these two parameters to explore the convective boundary layer flow past a vertical plate. Khan and Pop [17] extend the work of Kuznetsov and Nield [18] and investigated the impact of nanoparticle fraction of nanofluids in stretching surfaces. Anwar *et al.,* [19] conducted a study on non-linear stretching sheet and evaluated an impact of transmission of heat and mass in nanofluids.

Numerous studies conducted over the last several decades have established the presence of multiple solutions for boundary layer flows associated with moving surfaces. Carragher and Crane [7] pioneered the analytical solution of boundary layer fluid flow across stretching sheet. Sakiadis [29] further investigated the effect on a moving plate. Bachok *et al.,* [3] examined the boundary-layer flow over a moving flat plate. Later, Roşca and Pop [28] explored boundary layer flow on a moving surface by using nanofluid model developed by Buongiorno [6]. Mohamed *et al.,* [23] studied Boundary layer flow on moving plate with viscous dissipation in nanofluid. Zulkifli *et al.,* [35] revised and investigated the problem presented by Mohamed *et al.,* [23] using Buongiorno's model.

The study of fluid flow on moving surfaces was expanded to include other surfaces and also the influence of numerous parameters. Bhattacharyya *et al.,* [5] studied the impact of partial slip and heat transfer on shrinking sheet. Noghrehabadi *et al.,* [24] explored the impact of same parameters on stretching surface when nanoparticle fractions were present. A study on mixed convection and mass transmission effects over stretching sheet was conducted by Mishra and Singh [21]. Ramya *et al.,* [26] further evaluated the influence of MHD viscous flow and heat transfer. Next, Raza [27] explored the role of thermal radiation and velocity slip in MHD Casson fluid. In addition to previous studies, Daniel *et al.,* [9] further added the effect of viscous dissipation and chemical reaction in his study. Ashgar and Ying [2] studied hybrid nanofluid flow with rotating stretching/shrinking sheet under the influence of magnetic field and Joule heating.

According to a literature assessment of the viscous dissipation effect, Gebhart [10] explored boundary-layer analysis of the impacts of viscous dissipation for external flow. Later, the impact of viscous dissipative heat on convective flow past a vertical plate were investigated in a study of Soundalgekar [30]. Vajravelu and Hadjinicolaou [32] examined the same effects with internal heat generation on stretching sheet. Partha *et al.,* [25] further extended the study on mixed convection flow on exponentially stretching surface. Ishak *et al.,* [12] investigated boundary layer flow through moving wall. Balla and Naikoti [4] studied chemical reaction and radiation across vertical plate. Reddy *et al.,* [14] examined MHD convection flow in vertical plate with viscous dissipation. Khan *et al.,* [16] investigated the magnetohydrodynamic (MHD) flow of a double stratified micropolar fluid across a vertical stretching/shrinking sheet in the presence of suction, chemical reaction, heat source effects. Jahan *et al.,* [13] examined the simulations influence of exponential solar radiation and dissipative transport of steady mixed convective hybrid nanofluid.

Finite Difference Method have dominated the Computational Fluid Dynamics due to its simplicity in formulations and computations Yang *et al.,* [34]. Various researchers have contributed in reporting efficiency of FDM in solving second order differential equations. Blottner [20] solved the Levy-Lees form of the laminar boundary layer equations with several second-order accurate finite-difference schemes for incompressible flow. Ibrahim and Shanker [11] applied implicit finite difference technique to investigate unsteady laminar (MHDs) boundary layer flow with magnetic field and a thermal effect. Khader and Megahed [15] employed the finite difference approach to examine the impact of heat transmission and thermal radiation on stretching sheet. Therefore, FDM was employed as a numerical simulation method in this research.

The purpose of this research is to further contribute to the existing studies conducted by Mohamed *et al.,* [23] and Zulkifli *et al.,* [35]. The influence of slip conditions, viscous dissipation and magnetic field on boundary layer flow on moving plate will be considered in this research. To the best of our knowledge, this is the first study to investigate the effect of slip and magnetic field on

boundary layer flow past a moving plate. As a result, we expect that the current work will make a significant contribution to future research.

2. Mathematical Formulation

The influence of transverse magnetic field, viscous dissipation and slip conditions on a steady two dimensional incompressible laminar boundary layer flow across a moving plate in nanofluid is investigated. At time t $= 0$ the plate velocity is considered to be $u_w(x) = \varepsilon U_\infty$ in an external free stream of uniform velocity U_∞, where ε is a parameter describing the plate velocity [33]. It is considered that Flow occurs at y ≥ 0, in which y is the perpendicular to the moving plate. The components of velocity u and v are situated on x and y axis, correspondingly. T is considered to represent the temperature within boundary layer, T_w is temperature at wall and T_∞ be ambient temperature. Volume fraction of nanoparticles is assumed to be C, C_w is defined as volume fraction of nanoparticles at wall and C_∞ be volume fraction of ambient nanoparticle. A traverse magnetic field B_0 is applied in the direction of x. Figure 1 demonstrates geometry of the problem.

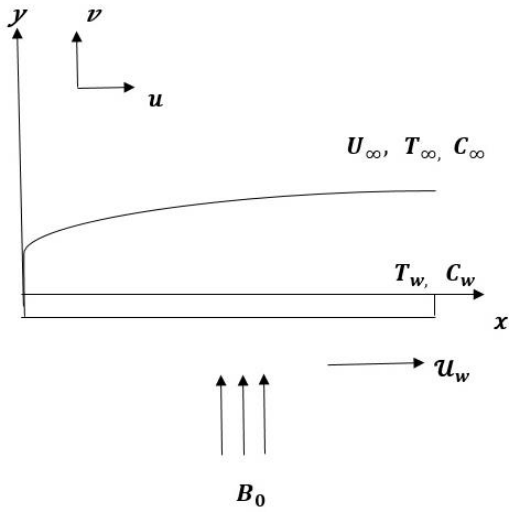

Fig. 1. Physical Model of problem

Based on studies mentioned above and according to Khan and Pop [17], Bachok *et al.,* [3], Roşca and Pop [28], Mohamed *et al.,* [23], Zulkifli *et al.,* [35], governing equations can be written as:

$$\frac{\partial u}{\partial x} + \frac{\partial v}{\partial y} = 0 \tag{1}$$

$$u\frac{\partial u}{\partial x} + v\frac{\partial u}{\partial y} = \nu\frac{\partial^2 u}{\partial y^2} - \frac{\sigma B_0^2}{\rho}u \tag{2}$$

$$u\frac{\partial T}{\partial x} + v\frac{\partial T}{\partial y} = \frac{k}{\rho C_p}\frac{\partial^2 T}{\partial y^2} + \tau\left(D_B\ \frac{\partial C}{\partial y}\frac{\partial T}{\partial y} + \frac{D_T}{T_\infty}\left(\frac{\partial T}{\partial y}\right)^2\right) + \frac{\mu}{\rho C_p}\left(\frac{\partial u}{\partial y}\right)^2 \tag{3}$$

$$u\frac{\partial C}{\partial x} + v\frac{\partial C}{\partial y} = D_B\frac{\partial^2 C}{\partial y^2} + \frac{D_T}{T_\infty}\frac{\partial^2 T}{\partial y^2} \tag{4}$$

Subjected to the boundary conditions

$$\begin{cases} v = V_0,\ u = \varepsilon U_\infty + N_1 \frac{\partial u}{\partial y},\ T = T_\infty + N_2 \frac{\partial T}{\partial y}\ ,\ C = C_\infty + N_3 \frac{\partial C}{\partial y}, & at\ \ y = 0 \\ u \to U_\infty,\ T \to T_\infty,\ C \to C_\infty, & at\ \ y \to \infty \end{cases} \tag{5}$$

Where u and v denote the x- and y-direction velocity components, respectively, ρ signifies the fluid density, μ indicates the dynamic velocity, $v(=\frac{m}{r})$ represents the kinematic viscosity, k is considered as thermal conductivity and C_p denotes specific heat capacity. Additionally, D_T and D_B are thermophoresis and Brownian diffusion coefficients, respectively. Moreover, $N_1, N_2\ and\ N_3$ are velocity, temperature and concentration slip coefficient respectively.

Eq. (1) to Eq. (4) subjected to boundary conditions (5) are defining similarity transformation as follow

$$\begin{aligned} &\eta = \left(\frac{U_\infty}{2\nu x}\right)^{1/2} y, \psi = \ (2U_\infty \nu x)^{1/2} f(\eta) \\ &T = T_\infty + (T_w - T_\infty)\theta(\eta) \\ &C = C_\infty + (C_w - C_\infty)\phi(\eta) \\ &\theta(\eta) = \frac{T - T_\infty}{T_w - T_\infty}, \phi(\eta) = \frac{C - C_\infty}{C_w - C_\infty} \end{aligned} \tag{6}$$

Where θ and ϕ denote dimensionless temperature and resealed nanoparticle volume fraction respectively. Stream function ψ is assumed as $u = \frac{\partial \psi}{\partial y}$ and $v = \ -\frac{\partial \psi}{\partial x}$, as a result of

$$u = U_\infty f'(\eta) \tag{7}$$

$$v = \ -\left(\frac{U_\infty \nu}{2x}\right)^{\frac{1}{2}} f(\eta) + \frac{U_\infty y}{2x} f'(\eta) \tag{8}$$

By applying the similarity transformation to Eq. (2) through Eq. (5), the resulting equations are as follows:

$$f''' + \ ff'' - Mf' = 0 \tag{9}$$

$$\frac{1}{P_r}\theta'' + f\theta' + N_b\theta'\phi' + N_t\theta'^2 + Ecf''^2 = 0 \tag{10}$$

$$\phi'' + \frac{N_t}{N_b}\theta'' + Lef\phi' = \ 0 \tag{11}$$

Where $Pr = \frac{v\rho C_p}{k}$ represents the Prandtl number, $N_b = \frac{\tau D_B (C_w - C_\infty)}{v}$ denotes the Brownian motion parameter, $N_t = \frac{\tau D_T (T_w - T_\infty)}{T_\infty v}$ signifies thermophoresis parameter, $Ec = \frac{(U_\infty)^2}{C_p (T_w - T_\infty)}$ indicates Eckert number and $Le = \frac{v}{D_B}$ is given by the Lewis number, M $= \frac{2x\sigma B_0^2}{\rho U_\infty}$ is defined as the magnetic parameter.

Corresponding boundary conditions

$$\begin{cases} f(\eta) = V_0,\ f'(\eta) = \varepsilon + \delta f''(\eta),\ \theta(\eta)\ = 1 + \lambda\theta'(\eta)\ ,\ \phi(\eta)\ = 1 + \gamma\phi'(\eta), & at\ \ \eta = 0 \\ f'(\infty) \to 1,\ \theta(\infty) \to 0,\ \phi(\infty) \to 0, & at\ \eta \to \infty \end{cases} \quad (12)$$

Note that $\delta = N_1 \left(\frac{U_\infty}{2\nu x}\right)^{\frac{1}{2}}$ is the velocity slip, $\lambda = N_2 \left(\frac{U_\infty}{2\nu x}\right)^{\frac{1}{2}}$ thermal slip and $\gamma = N_3 \left(\frac{U_\infty}{2\nu x}\right)^{\frac{1}{2}}$is the concentration slip parameter. The Physical quantities, C_f,Nu_x and Sh_x are given by

$$C_f = \frac{\tau_w}{\rho u_e^2}, Nu_x\ = \frac{x q_w}{k(T_w - T_\infty)}, Sh_x = \frac{x j_w}{D_B(C_w - C_\infty)}. \quad (13)$$

The shear stress, heat flux and mass flux on surface are denoted by τ_w , q_w , j_w respectively and also shown as

$$\tau_w = \mu \left(\frac{\partial u}{\partial y}\right)_{y=0}, q_w = -k \left(\frac{\partial T}{\partial y}\right)_{y=0}, j_w = -D_B \left(\frac{\partial C}{\partial y}\right)_{y=0} \quad (14)$$

where μ = ρv is the dynamic viscosity.

By applying the similarity variables in Eq. (6), following relation are obtained

$$C_f (2Re_x)^{1/2} = f^{"}(0),\ Nu_x \left(\frac{Re_x}{2}\right)^{-1/2} = -\theta'\,(0), Sh_x \left(\frac{Re_x}{2}\right)^{-1/2} = -\emptyset'(0) \quad (15)$$

Where $\mathrm{R}e_x = \frac{U_\infty x}{\nu}$ is local Reynolds number and $(2Re_x)^{1/2}, Nu_x \left(\frac{Re_x}{2}\right)^{-1/2} and\ Sh_x \left(\frac{Re_x}{2}\right)^{-1/2}$ are defined by reduced C_{fr}, Nur and Shr and also given as $f"(0), -\theta'(0)\ and - \emptyset'(0)$, respectively.

3. Method of Solution

To solve Eq. (9) to Eq. (11) along with the boundary conditions (12), we will transform the third order derivative into second order derivative by replacing $f' = F$.

Then the above system of equation will become

$$f' = F \quad (16)$$

$$F'' + fF' - MF = 0 \quad (17)$$

$$\theta'' + P_r f\theta' + P_r N_b \theta'\phi' + P_r N_t \theta'^2 + P_r Ec F'^2 = 0 \quad (18)$$

$$\phi'' + \frac{N_t}{N_b}\theta'' + L_e f\phi' = 0 \quad (19)$$

Corresponding boundary conditions will be transformed to

$$\begin{cases} f(\eta) = V_0,\ F(\eta) = \varepsilon + \delta F'(\eta),\ \theta(\eta)\ = \lambda\theta'(\eta)\ ,\ \phi(\eta)\ = \gamma\phi'(\eta), & at\ \ \eta = 0 \\ F(\eta) \to 1,\ \theta(\eta) \to 0,\ \phi(\eta) \to 0, & at\ \ \ \eta \to \infty \end{cases} \quad (20)$$

System (16) to (19) is nonlinear one. To obtain solution of this system, it is firstly required to convert these equations into a system of linear differential equation. This is done by Newton linearization method. Eq. (16) is linear in variable f, therefore, it is not necessary to make it linear. We will make Eq. (16) linear in variable F, while taking all other variables constants. Same will be done for Eq. (18). Eq. (19), however, is linear in variable ϕ.

Linear Eq. (18) and Eq. (19) will be solved as linear second order differential equation iteratively [34]. Thus, the resulting system of equations is as follow

$$\begin{cases} f' = F \\ F''_{n+1} + (A_F)_n\, F'_{n+1} + (B_F)_n\, F_{n+1} = (D_F)_n \\ \theta''_{n+1} + (A_\theta)_n\, \theta'_{n+1} + (B_\theta)_n\, \theta_{n+1} = (D_\theta)_n \\ \phi'' + \frac{N_t}{N_b}\theta'' + L_e f \phi' = 0 \end{cases} \tag{21}$$

Along with the boundary conditions

$$\begin{cases} f = V_0,\ F(\eta) = \varepsilon + \delta F'(\eta),\ \theta(\eta) = \lambda\, \theta'(\eta),\ \phi(\eta) = \gamma\, \phi'(\eta), & at\ \ \eta = 0 \\ F \to 0,\ \theta \to 0,\ \phi \to 0, & at\ \ \eta \to \infty \end{cases} \tag{22}$$

Eq. (21) along with Eq. (22) will be solved by Finite Difference method (FDM). The first equation is straight forward, replacing derivative in first equation of (21) by their corresponding center finite difference approximation.

$\frac{f_{i+1}-f_i}{2\Delta\eta} = F_i$ (Order of accuracy of this difference formula is one)

This implies that

$$f_{i+1} = f_i + 2\Delta\eta\, F_i \tag{23}$$

with $f_1 = V_w$ (the boundary conditions).

Now for the second equation, finite difference method is used for linear second order equation. Before that, we need to evaluate the coefficients $(A_F)_n$, $(B_F)_n$ and $(D_F)_n$ at each node of the given domain but at previous iteration n

$$(A_F)_n = (f_i)_n \tag{24}$$

With $i = 2\ to\ N$, the subscript n represent the previous iteration and i is for interior nodes only. We will require an initial guess to start the iterations process.

$$\begin{aligned} (B_F)_n &= -4(F_i)_n + M \\ (D_F)_n &= -fF' + MF - 4F_n\, F_n + f\, F'_n \end{aligned} \tag{25}$$

Derivative in the above approximation is replaced by the second order center difference approximation, thus D_n will become

$$(D_F)_n = -\left(\frac{f_i(F_{i+1}-F_{i-1})}{2\Delta\eta}\right)_n + M(F_i)_n - 4(F_i)_n\,(F_i)_n + \left(\frac{f_i(F_{i+1}-F_{i-1})}{2\Delta\eta}\right)_n \tag{26}$$

After knowing $(A_F)_n$, $(B_F)_n$ and $(D_F)_n$ at each node of the domain, we can now use the finite difference approximation for the second order linear differential equation.

$$F''_{n+1}(\eta) + (A_F)_n F'_{n+1}(\eta) + (B_F)_n F(\eta) = (D_F)_n$$

$(A_F)_n, (B_F)_n$ and $(D_F)_n$ in above equation are just constants now. We have to solve it as a linear second order differential equation. Writing above equation at a general node i

$$(F_i)''_{n+1} + \left(A_{F_i}\right)_n (F_i)'_{n+1} + \left(B_{F_i}\right)_n (F_i)_{n+1} = \left(D_{F_i}\right)_n$$

Replacing the derivatives in the above equation by their second order center finite difference approximation, equation will become

$$a_i (F_{i-1})_{n+1} + b_i (F_i)_{n+1} + c_i (F_{i+1})_{n+1} = r_i \tag{27}$$

With the corresponding boundary conditions

$$\begin{cases} F_0 = c + \frac{(F_1 - F_0)}{\mathrm{h}} \\ F(\eta \to \infty) = F_b \end{cases} \tag{28}$$

In finite difference form, above boundary conditions are written as follow

$$F_0 = c + \frac{(F_1 - F_0)}{\mathrm{h}}$$

$$\left(c + \frac{1}{h}\right) F_0 - \frac{1}{h} F_1 = 1$$

$$\begin{cases} \left(c + \frac{1}{h}\right) F_0 - \frac{1}{h} F_1 = 1 \\ F_N = F_b \end{cases} \tag{29}$$

For $= 1,2,3, \ldots N-1$, Eq. (27) will be converted into a set of algebraic linear equations. Resulting system is further computed by using LU decomposition and Matlab software. All of the results were in excellent agreement.

4. Results and Discussion

In the current study, a numerical computation method has been carried using Finite difference method with slip conditions parameters (δ, λ, γ) and magnetic field parameter (M) applied on moving plate in a nanofluid showing viscous dissipation. Pr, ε, $\mathrm{N_b}$, $\mathrm{N_t}$,Ec, and Le are considered as fluid flow parameters. Based on the literature survey, Le is investigated in the range 1 to 20, while $\mathrm{N_b}$,$\mathrm{N_t}$ and Ec are considered in the range 0.1 to 0.5 [17,35]. Table 1 to Table 3 and Figure 2 to Figure 23 demonstrate the numerical findings depicting the influence parameters on coefficient of local skin friction $-\mathrm{C_{fr}}\,(2\mathrm{Re_x})^{1/2}$, Local Nusselt number $\mathrm{Nu_x}\left(\frac{\mathrm{Re_x}}{2}\right)^{-\frac{1}{2}}$and Sherwood number $\mathrm{Sh_x}\left(\frac{\mathrm{Re_x}}{2}\right)^{-1/2}$.

Table 1
Comparing the Numerical values of $\mathrm{Nu_x}\sqrt{\mathrm{Re_x}}$ or $(-\theta'(0)/\sqrt{2})$ (With regard to different values of Pr for $\epsilon = \mathrm{N_b} = \mathrm{N_t} = \mathrm{Ec} = \mathrm{Le} = 0$

Pr	Bejan [1]	Roşca and Pop [28]	Mohamed *et al.,* [23]	Zulkifli *et al.,* [35]	Present Results
0.7	0.292	0.29268	0.292680	0.292680	0.293330106
0.8	0.307	0.30691	0.306917	0.306917	0.307487479
1	0.332	0.33205	0.332057	0.332057	0.332621772
5	0.585	0.57668	0.576689	0.576689	0.578169594
10	0.730	0.72814	0.728141	0.728141	0.730411717

To verify the correctness and validity of the obtained results, the values of $-\theta'(0)/\sqrt{2})$ for $\epsilon = \mathrm{N_b} = \mathrm{N_t} = \mathrm{Ec} = \mathrm{Le} = 0$ with altered values of Pr (Prandtl Number) was calculated. The obtained values are compared to those reported by Bejan [1], Roşca and Pop [28], Mohamed *et al.*, [23] and Zulkifli *et al.*, [35], as indicated through Table 1. Obtained numerical values using the present numerical method exhibit an excellent agreement with the prior studies.

The impacts of various fluid flow parameters on reduced skin friction coefficient, Nusselt number and Sherwood number are exhibited in Table 2. It is clearly noticed that C_{fr} is highlighting for improving value of M but shows a reverse behavior w.r.t. δ and ε. Thus, analysis of data demonstrates that magnetic fields increase skin friction, but velocity slip (δ) and plate velocity parameter (ϵ) have the opposite impact. It's because skin friction rises in the presence of a magnetic field due to the resistance provided by the Lorentz force. Moreover, when the velocity slip increases, the fluid's adhesive force to the surface reduces, resulting in a decrease in skin friction. Furthermore, it is recognized that Nur is reduced with steadily rising values M, δ, λ but the opposite behavior is observed with an increase in γ and ϵ. The study of tabular figures reveals that when M, δ, λ and γ increase, the local Sherwood number falls, while it rises for larger values of.

Table 3 reveals the variance of Nur, Shr for different values of Pr, Nb, Nt, Ec and Le when $\delta = \lambda = \gamma = 1$, $\mathrm{M} = 1.5, \epsilon = 0.5$. Nur is demonstrated to be a reducing function of the Nb, Nt, Ec and Le, parameters, whereas Shr shows an increase for same parameters. However, reverse phenomena is observed for Pr.

Table 2
Numerical values of local skin friction coefficient, reduced Nusselt number and reduced Sherwood number for different parameters with $\mathrm{N_b} = \mathrm{N_t} = \mathrm{Ec} = 0.1, \mathrm{Le} = 10, \mathrm{Pr} = 7$

M	δ	λ	γ	ϵ	C_{fr}	Nur	Shr
1	1.0	1.0	1.0	0.5	-0.0918	0.4852	0.5653
1.5	1.0	1.0	1.0	0.5	-0.1652	0.4447	0.5455
2	1.0	1.0	1.0	0.5	-0.2140	0.4109	0.5317
1.5	2.0	1.0	1.0	0.5	-0.1065	0.4295	0.5375
1.5	3.0	1.0	1.0	0.5	-0.0787	0.4216	0.5337
1.5	4.0	1.0	1.0	0.5	-0.0625	0.4169	0.5315
1.5	1.0	2.0	1.0	0.5	-0.1652	0.3089	0.5579
1.5	1.0	3.0	1.0	0.5	-0.1652	0.2358	0.5652
1.5	1.0	4.0	1.0	0.5	-0.1652	0.1894	0.5711
1.5	1.0	1.0	2.0	0.5	-0.1652	0.4586	0.3388
1.5	1.0	1.0	3.0	0.5	-0.1652	0.4586	0.2473
1.5	1.0	1.0	4.0	0.5	-0.1652	0.4652	0.1934
1.5	1.0	1.0	1.0	0.1	0.0555	0.3774	0.5160
1.5	1.0	1.0	1.0	0.5	-0.1652	0.4447	0.5455
1.5	1.0	1.0	1.0	1.0	-0.4463	0.4966	0.5835

Table 3
Numerical values of reduced Nusselt number and reduced Sherwood number for different parameters with $\delta = \lambda = \gamma = 1$, $M = 1.5, \epsilon = 0.5$

Pr	Nb	Nt	Ec	Le	Nur	Shr
3	0.1	0.1	0.1	10	0.4032	0.5590
5	0.1	0.1	0.1	10	0.4286	0.5503
7	0.1	0.1	0.1	10	0.4443	0.5458
7	0.1	0.1	0.1	10	0.4447	0.5455
7	0.3	0.1	0.1	10	0.3640	0.5883
7	0.5	0.1	0.1	10	0.2803	0.5971
7	0.1	0.1	0.1	10	0.4447	0.5455
7	0.1	0.3	0.1	10	0.3566	0.5835
7	0.1	0.5	0.1	10	0.2857	0.7219
7	0.1	0.1	0.1	10	0.4447	0.5455
7	0.1	0.1	0.2	10	0.4245	0.5549
7	0.1	0.1	0.3	10	0.4035	0.5647
7	0.1	0.1	0.1	8	0.4451	0.5121
7	0.1	0.1	0.1	10	0.4451	0.5451
7	0.1	0.1	0.1	12	0.4446	0.5722

The impact of the magnetic field on velocity parameter is depicted in Figure 2. An increase in magnetic field combined with a slip condition causes the fluid velocity to reduce. This results as the Lorentz force is activated in the presence of a transverse magnetic field, which reduces fluid velocity. The Lorentz force increases as the magnetic field increases, causing a decrease in fluid velocity.

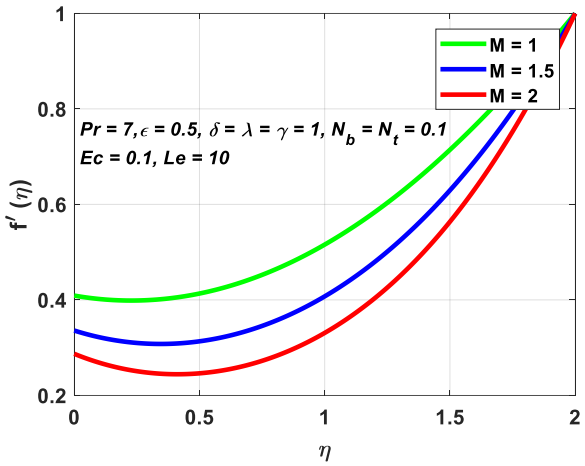

Fig. 2. Variation of velocity $f'(\eta)$ with η with several values of M

Figure 3 illustrates that when the value of M rises, so does the concentration of nanoparticles. This effect is noticed because of the Lorentz force, that being a resistant force retards the fluid velocity, causing heat production. As a result, under the influence of strong magnetic field, thermal boundary layer thicknesses and nanoparticle concentration increase.

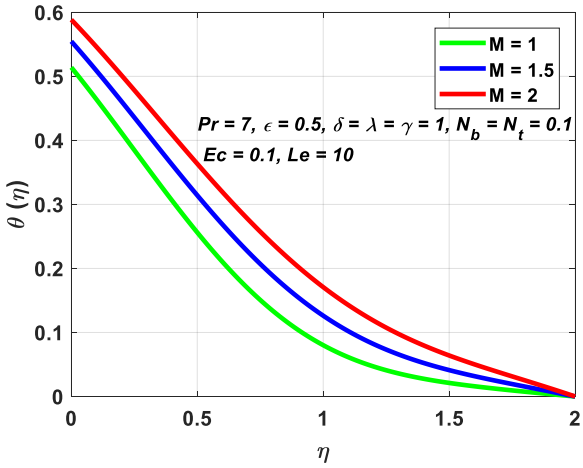

Fig. 3. Variation of temperature θ (η) with η with several values of M

Figure 4 highlights that there is a negligible effect of increase in Lewis number on temperature. This is because as the Lewis number increases, so does the Brownian diffusion coefficient, and vice versa. In the present study, zero nanoparticle condition is applied, hence, Lewis number (Le), has no impact on the temperature profile. Figure 5 describes the impact of Le on dimensionless concentration. With larger Le values, nanoparticle volume fraction is shown to be significantly reduced. Raising the Lewis number increases the thickness of thermal boundary layer while decreasing the concentration, as illustrated in Figure 6.

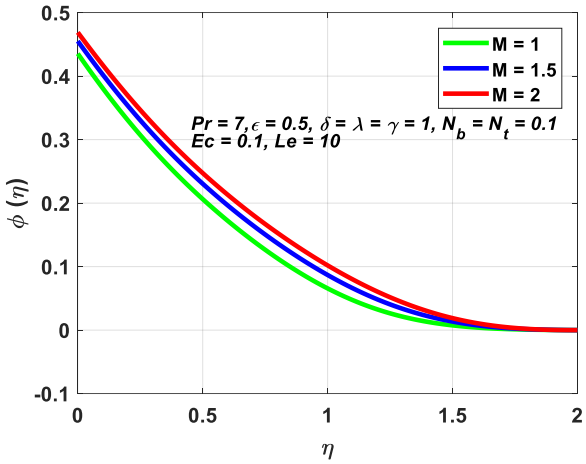

Fig. 4. Variation of concentration ϕ (η) with η with several values of M

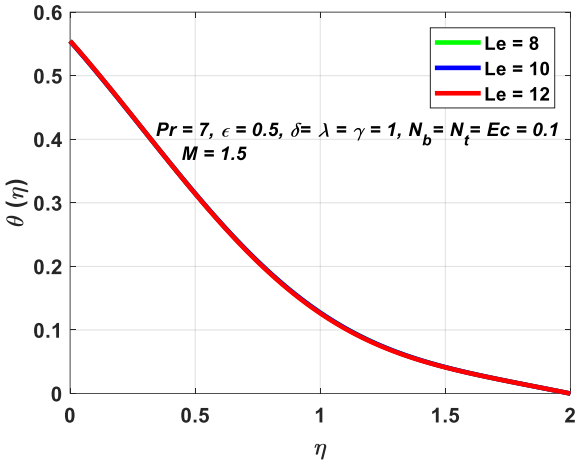

Fig. 5. Variation of temperature θ (η) with η with several values of Le

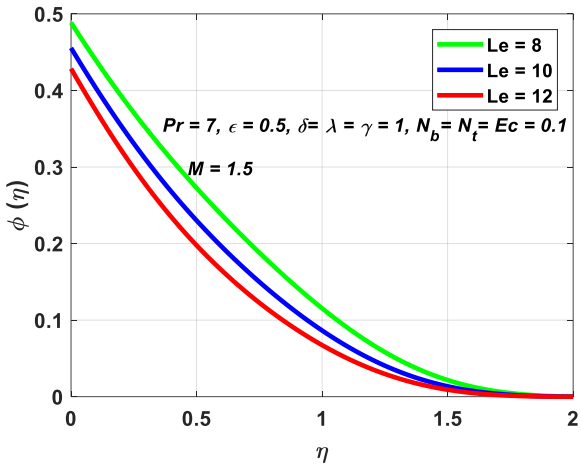

Fig. 6. Variation of concentration ϕ (η) with η with several values of Le

The influence of viscous dissipation parameter on the temperature profile as illustrated in Figure 7. As reported in studies, an increase in Ec number indicates a favorable effect on boundary layer temperature, resulting in a temperature increase associated with the increase in Ec. Increases in viscous dissipation (Ec) also result in increase in thickness of the thermal boundary layer, as presented in Figure 8.

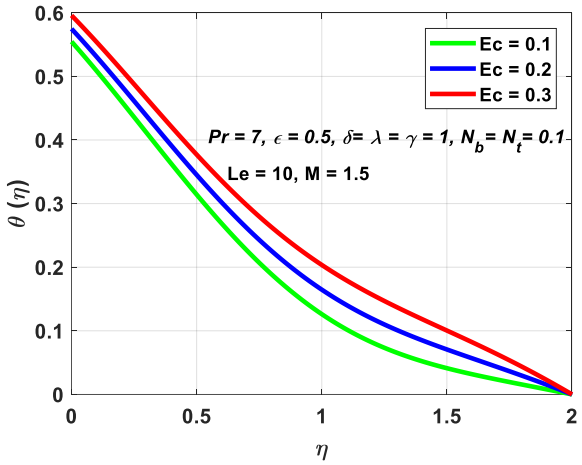

Fig. 7. Variation of temperature θ (η) with η with several values of Ec

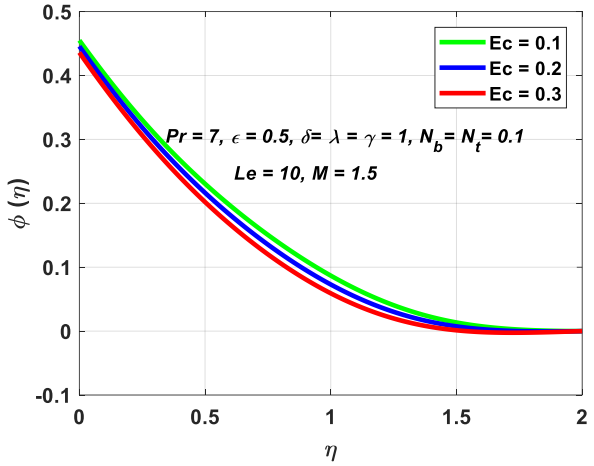

Fig. 8. Variation of concentration ϕ (η) with η with several values of Ec

As demonstrated in Figure 9 and Figure 10, a rise in ε causes an increase in velocity profile while a drop in temperature profile. As value of the plate velocity parameter (ε > 0) rises, thickness of thermal boundary layer reduces, that is depicted in Figure 11. This is because a rise in ε leads to a rise in ratio between the plate and fluid velocity. This difference in velocities enables the fluid to flow through the region more quickly, reducing the thickness of thermal boundary layer.

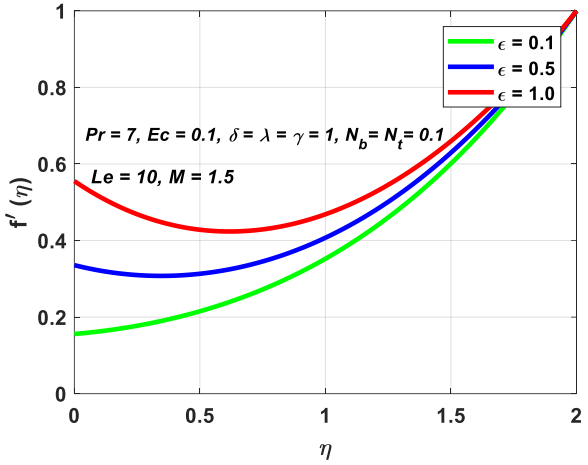

Fig. 9. Variation of velocity $f'(\eta)$ with η with several values of ε

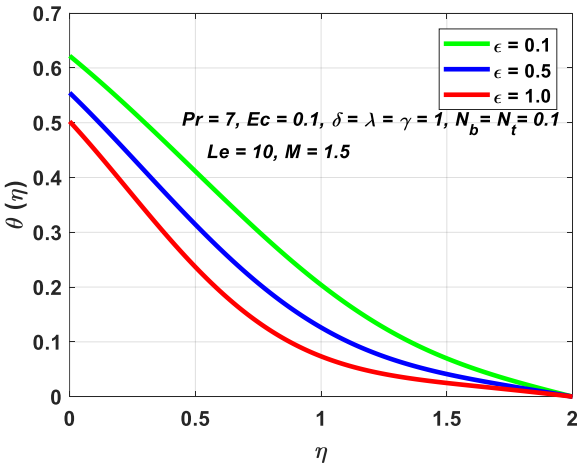

Fig. 10. Variation of temperature $\theta(\eta)$ with η with several values of ε

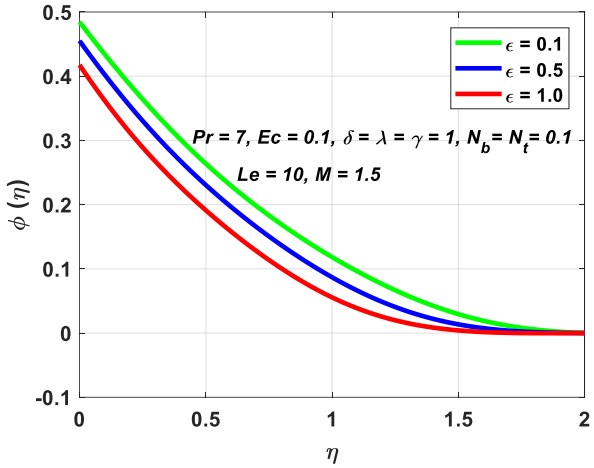

Fig. 11. Variation of concentration $\phi(\eta)$ with η with several values of ε

Figure 12 showed the impact of Prandtl number on temperature profile. The Pr is the characteristic of fluids that indicates that a fluid having a low Pr value has more thermal diffusivity in principle. As a result of this phenomenon, increasing the Prandtl number results in decreased in temperature and thickness of thermal boundary layer, as indicated in Figure 13.

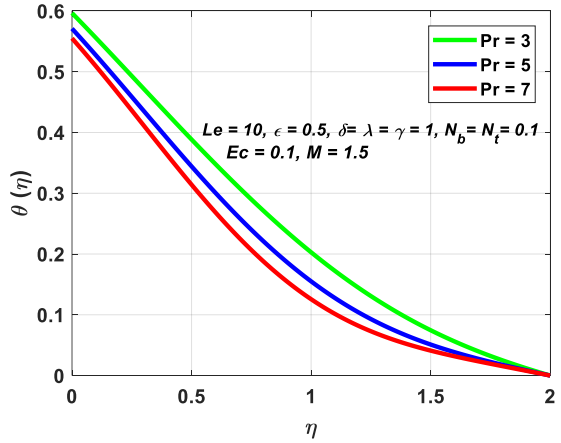

Fig. 12. Variation of temperature $\theta(\eta)$ with η with several values of Pr

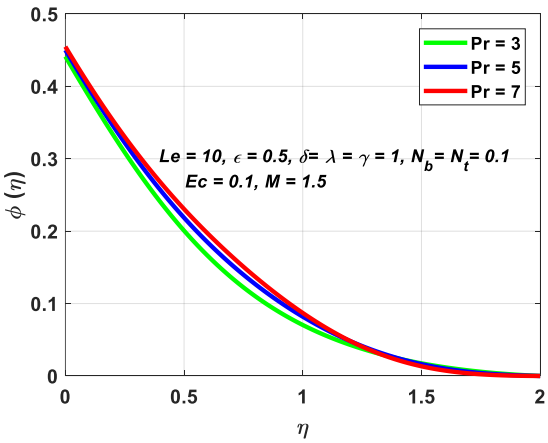

Fig. 13. Variation of concentration $\phi(\eta)$ with η with several values of Pr

Impacts of Nb on the dimensionless temperature and concentration profiles are demonstrated in Figure 14 and Figure 15. As the Nb is increased, the temperature profile rises as exhibited in Figure 14, while the concentration profile falls as seen in Figure 15. It is supported by the phenomenon that a higher value of the Nb affects the thickening of thermal boundary layer to great extent. Volume fraction of nanoparticles reduces as Brownian motion increases.

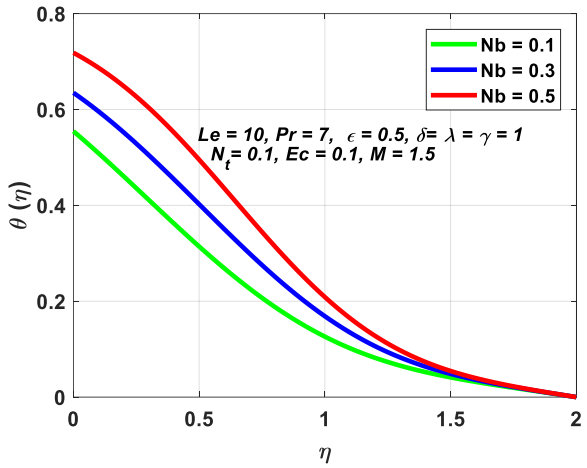

Fig. 14. Variation of temperature θ (η) with η with several values of N_b

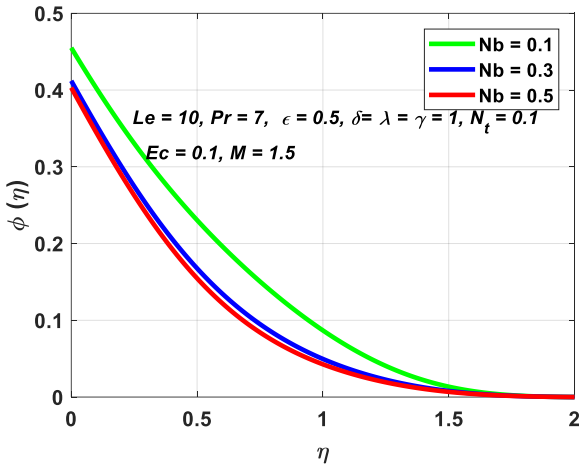

Fig. 15. Variation of concentration ϕ (η) with η with several values of N_b

Figure 16 depicts the thermal boundary layer thickness increases as the thermophoresis diffusion parameter (Nt) increases. It has been found that as thermophoresis rises, a large number of nanoparticles migrate from the hot zone to the cold region, the nanofluid temperature rises. Furthermore, as demonstrated in Figure 17, increasing the value of the Nt causes an increase in nanoparticle volume fraction. Thermophoretic force is generated by a thermal gradient that induces a flow away from the surface. As a result, the fluid becomes heated and moves away, thus increasing thickness of thermal boundary layer.

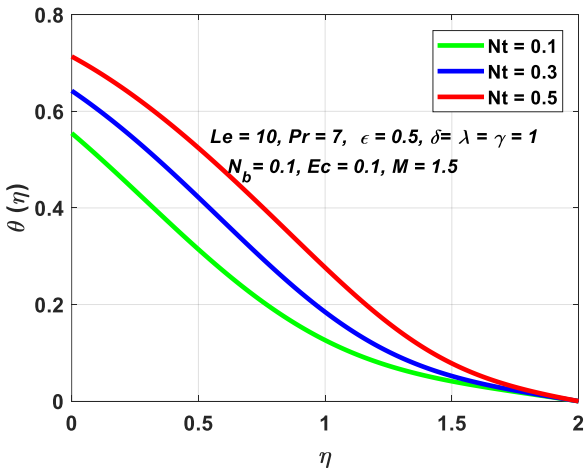

Fig. 16. Variation of temperature θ (η) with η with several values of N_t

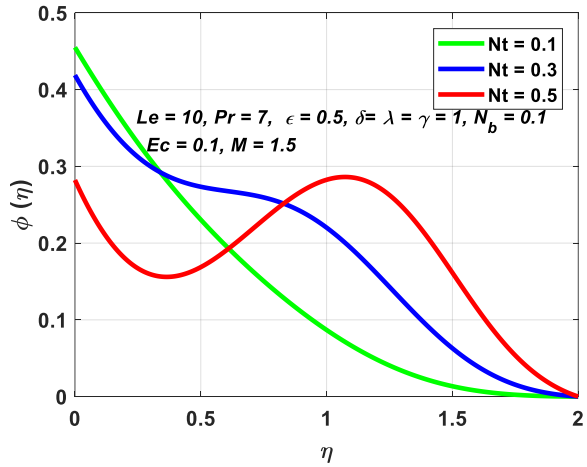

Fig. 17. Variation of concentration ϕ (η) with η with several values of N_t

Figure 18 shows that with rising levels of δ, velocity profile is shown to diminish. The slip velocity increases as δ is increased. As slip velocity increases, velocity of moving plate surface differs from velocity of flow near the plate, causing fluid velocity to drop. As a result, increasing the slip velocity parameter causes increase in slip velocity but decrease in fluid velocity.

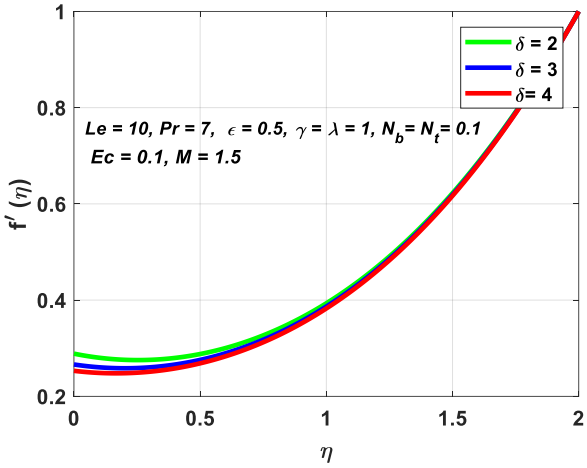

Fig. 18. Variation of velocity f′ (η) with η with several values of δ

Impact of velocity slip on temperature profile at boundary surface is depicted in Figure 19. Result shows that when slip parameter increases, so does the boundary surface temperature profile. It is because an increase in velocity slip induces diffusion of nanoparticles into the boundary layer, resulting in a more homogeneous concentration level of nanoparticles in the fluid, which raises the concentration boundary layer thickness, as illustrated in Figure 20.

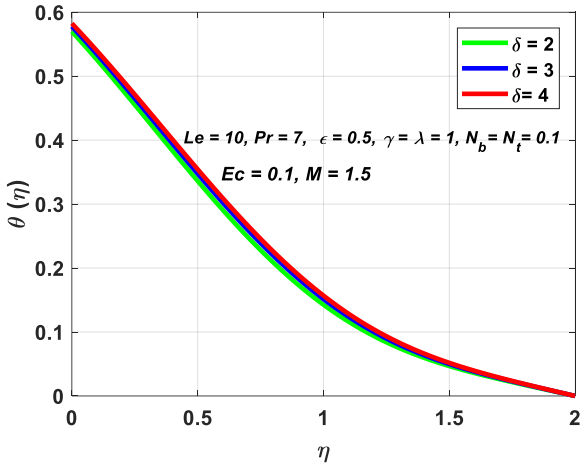

Fig. 19. Variation of temperature θ (η) with η with several values of δ

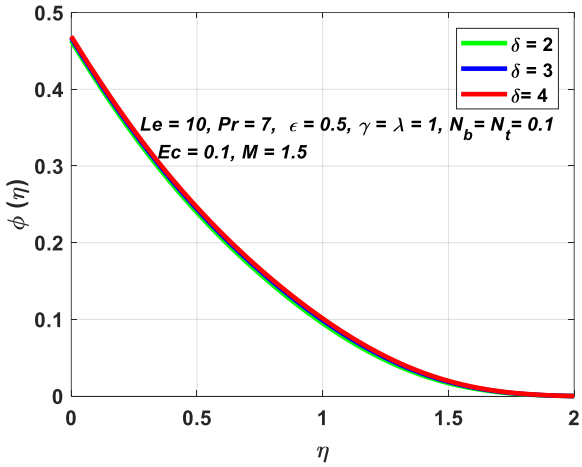

Fig. 20. Variation of concentration ϕ (η) with η with several values of δ

Figure 21 and Figure 22 examine the implications of λ on temperature and nanoparticle volume fraction. Thermal slip results in a decrease in the temperature profile. It is important to note that the influence of γ on the concentration profile quite resembles to that of λ on the temperature profile, as depicted in Figure 21 and Figure 24. This is because slip reduces the rate of fluid flow, resulting in a reduction in net molecular movement. Temperature and mass fraction both fall as a result of the reduced molecular mobility. It is hypothesized that if thermal slip parameter can regulate temperature inside the flow, the concentration slip parameter may be able to influence the mass transport phenomenon as well. The temperature profile and the concentration slip parameter exhibit an inverse relationship within the boundary layer region, as illustrated in Figure 23.

The purpose of present study was to explore combined impact of velocity, temperature, and concentration slip factors on boundary layer flow. It was determined that the thermal slip parameter has essentially identical effects to the concentration slip parameter. As a result, thermal and

concentration boundary layers can be controlled to desired values by modifying the thermal and concentration slip parameters.

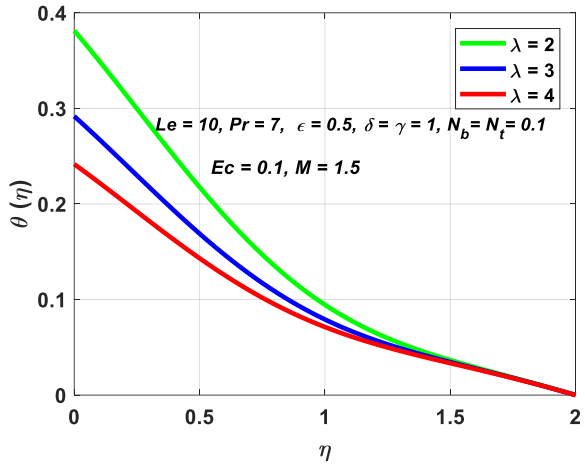

Fig. 21. Variation of temperature θ (η) with η with several values of λ

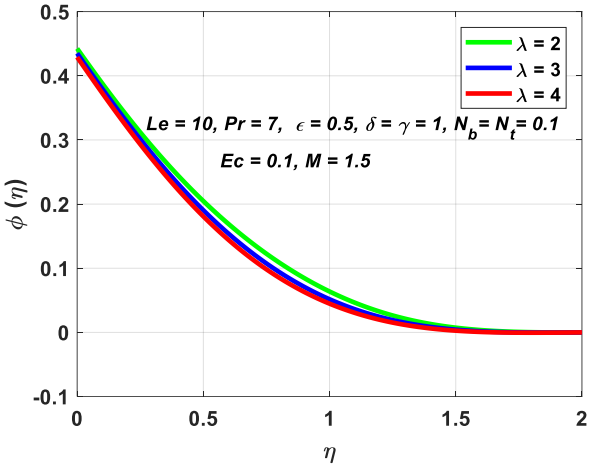

Fig. 22. Variation of concentration ϕ (η) with η with several values of λ

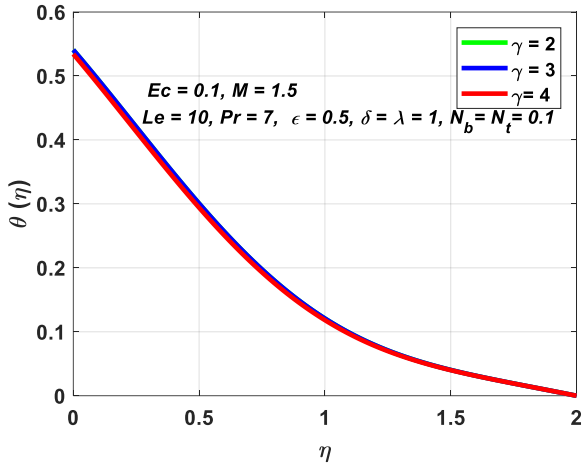

Fig. 23. Variation of temperature θ (η) with η with several values of γ

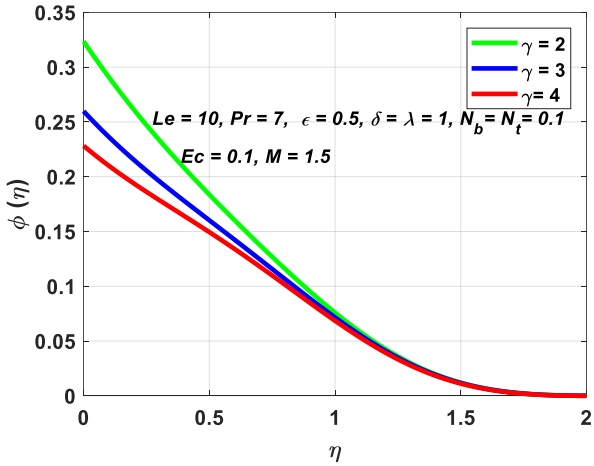

Fig. 24. Variation of concentration ϕ (η) with η with several values of γ

5. Conclusions

The numerical study of the boundary layer flow of a nanofluid across a moving plate with the effects of velocity slip, temperature slip, concentration slip, magnetic field, and viscous dissipation. The impacts of fluid flow factors on velocity, temperature, and concentration profile are investigated. M, δ, λ, γ, Ec, Le, Nb, Nt, Pr and ε are studied on different profiles. The results are as follows

i. The Lorentz force causes the velocity profile to decrease as the magnetic parameter M is increased, while temperature and concentration profiles increase.
ii. With existence of viscous dissipation, temperature profile rises. Moreover, nanoparticle volume fraction was reduced.
iii. When plate velocity parameter ε is increased, the velocity profile is enhanced while the temperature and concentration profiles are diminished.
iv. For Rrising values of δ, temperature profile rises and velocity profile drops. It also increases thickness of concentration boundary layer.

v. Temperature reduces and concentration rises when thermal slip parameter is enhanced.
vi. Temperatures increase and concentration reduces as concentration slip parameter is increased.
vii. Temperature drops and concentration increases as the Browinian motion parameter Nb and thermophoresis parameter Nt are increased.
viii. When Le increases, concentration profile increases.
ix. Increasing Prandtl number, decreases the temperature and concentration profile.

Acknowledgement
This research was not funded by any grant.

References

[1] Bejan, Adrian. *Convection heat transfer*. John Wiley & Sons, 2013. https://doi.org/10.1002/9781118671627
[2] Ashgar, Adnan, and The Yuan Ying. "Three Dimensional MHD Hybrid Nanofluid Flow with Rotating Stretching/Shrinking Sheet and Joule Heating." *CFD Letters* 13, no. 8 (2021): 1-19. https://doi.org/10.37934/cfdl.13.8.119
[3] Bachok, Norfifah, Anuar Ishak, and Ioan Pop. "Boundary-layer flow of nanofluids over a moving surface in a flowing fluid." *International Journal of Thermal Sciences* 49, no. 9 (2010): 1663-1668. https://doi.org/10.1016/j.ijthermalsci.2010.01.026
[4] Balla, Chandra Shekar, and Kishan Naikoti. "Radiation effects on unsteady MHD convective heat and mass transfer past a vertical plate with chemical reaction and viscous dissipation." *Alexandria Engineering Journal* 54, no. 3 (2015): 661-671. https://doi.org/10.1016/j.aej.2015.04.013
[5] Bhattacharyya, Krishnendu, Swati Mukhopadhyay, and G. C. Layek. "Slip effects on boundary layer stagnation-point flow and heat transfer towards a shrinking sheet." *International Journal of Heat and Mass Transfer* 54, no. 1-3 (2011): 308-313. https://doi.org/10.1016/j.ijheatmasstransfer.2010.09.041
[6] Buongiorno, Jacopo. "Convective transport in nanofluids." *Journal of Heat Transfer* 128, no. 3 (2006): 240-250. https://doi.org/10.1115/1.2150834
[7] Carragher, P., and L. J. Crane. "Heat transfer on a continuous stretching sheet." *Zeitschrift Für Angewandte Mathematik Und Mechanik* 62, no. 10 (1982): 564-565. https://doi.org/10.1515/9783112546901-009
[8] Choi, S. US, and Jeffrey A. Eastman. *Enhancing thermal conductivity of fluids with nanoparticles*. No. ANL/MSD/CP-84938; CONF-951135-29. Argonne National Lab. (ANL), Argonne, IL (United States), 1995.
[9] Daniel, Yahaya Shagaiya, Zainal Abdul Aziz, Zuhaila Ismail, Arifah Bahar, and Faisal Salah. "Slip role for unsteady MHD mixed convection of nanofluid over stretching sheet with thermal radiation and electric field." *Indian Journal of Physics* 94, no. 2 (2020): 195-207. https://doi.org/10.1007/s12648-019-01474-y
[10] Gebhart, B. "Effects of viscous dissipation in natural convection." *Journal of Fluid Mechanics* 14, no. 2 (1962): 225-232. https://doi.org/10.1017/S0022112062001196
[11] Ibrahim, Wubshet, and B. Shanker. "Unsteady MHD boundary-layer flow and heat transfer due to stretching sheet in the presence of heat source or sink." *Computers & Fluids* 70 (2012): 21-28. https://doi.org/10.1016/j.compfluid.2012.08.019
[12] Ishak, Anuar, Roslinda Nazar, and Ioan Pop. "Boundary layer flow and heat transfer past a moving plate with suction and injection." In *AIP Conference Proceedings*, vol. 1602, no. 1, pp. 435-442. American Institute of Physics, 2014. https://doi.org/10.1063/1.4882522
[13] Jahan, Sultana, M. Ferdows, M. D. Shamshuddin, and Khairy Zaimi. "Effects of Solar Radiation and Viscous Dissipation on Mixed Convective Non-Isothermal Hybrid Nanofluid over Moving Thin Needle." *Journal of Advanced Research in Micro and Nano Engineering* 3, no. 1 (2021): 1-11.
[14] Reddy, G. Jithender, R. Srinivasa Raju, and J. Anand Rao. "Influence of viscous dissipation on unsteady MHD natural convective flow of Casson fluid over an oscillating vertical plate via FEM." *Ain Shams Engineering Journal* 9, no. 4 (2018): 1907-1915. https://doi.org/10.1016/j.asej.2016.10.012
[15] Khader, M. M., and Ahmed M. Megahed. "Numerical simulation using the finite difference method for the flow and heat transfer in a thin liquid film over an unsteady stretching sheet in a saturated porous medium in the presence of thermal radiation." *Journal of King Saud University-Engineering Sciences* 25, no. 1 (2013): 29-34. https://doi.org/10.1016/j.jksues.2011.10.002
[16] Khan, Ansab Azam, Khairy Zaimi, Suliadi Firdaus Sufahani, and Mohammad Ferdows. "MHD Mixed Convection Flow and Heat Transfer of a Dual Stratified Micropolar Fluid Over a Vertical Stretching/Shrinking Sheet With Suction,

Chemical Reaction and Heat Source." *CFD Letters* 12, no. 11 (2020): 106-120. https://doi.org/10.37934/cfdl.12.11.106120

[17] Khan, W. A., and I. Pop. "Boundary-layer flow of a nanofluid past a stretching sheet." *International Journal of Heat and Mass Transfer* 53, no. 11-12 (2010): 2477-2483. https://doi.org/10.1016/j.ijheatmasstransfer.2010.01.032

[18] Kuznetsov, A. V., and D. A. Nield. "Natural convective boundary-layer flow of a nanofluid past a vertical plate." *International Journal of Thermal Sciences* 49, no. 2 (2010): 243-247. https://doi.org/10.1016/j.ijthermalsci.2009.07.015

[19] Anwar, M. I., I. Khan, S. Sharidan, and M. Z. Salleh. "Conjugate effects of heat and mass transfer of nanofluids over a nonlinear stretching sheet." *International Journal of Physical Sciences* 7, no. 26 (2012): 4081-4092. https://doi.org/10.5897/IJPS12.358

[20] Blottner, F. G. "Investigation of some finite-difference techniques for solving the boundary layer equations." *Computer Methods in Applied Mechanics and Engineering* 6, no. 1 (1975): 1-30. https://doi.org/10.1016/0045-7825(75)90012-2

[21] Mishra, Upendra, and Gurminder Singh. "MHD mixed convection and mass transfer due to unsteady stretching sheet." *Heat Transfer-Asian Research* 43, no. 5 (2014): 447-458. https://doi.org/10.1002/htj.21088

[22] Mishra, Upendra, and Gurminder Singh. "Dual solutions of forced convection flow along a stretching sheet with variable thickness in presence of free stream and magnetic field." *Sains Malaysiana* 46, no. 2 (2017): 349-358. https://doi.org/10.17576/jsm-2017-4602-20

[23] Mohamed, Muhammad Khairul Anuar, Nor Aida Zuraimi Noar, M. Z. Salleh, and Anuar Ishak. "Mathematical model of boundary layer flow over a moving plate in a nanofluid with viscous dissipation." *Journal of Applied Fluid Mechanics* 9, no. 5 (2016): 2369-2377. https://doi.org/10.18869/acadpub.jafm.68.236.25247

[24] Noghrehabadi, Aminreza, Rashid Pourrajab, and Mohammad Ghalambaz. "Effect of partial slip boundary condition on the flow and heat transfer of nanofluids past stretching sheet prescribed constant wall temperature." *International Journal of Thermal Sciences* 54 (2012): 253-261. https://doi.org/10.1016/j.ijthermalsci.2011.11.017

[25] Partha, M. K., P. V. S. N. Murthy, and G. P. Rajasekhar. "Effect of viscous dissipation on the mixed convection heat transfer from an exponentially stretching surface." *Heat and Mass Transfer* 41, no. 4 (2005): 360-366. https://doi.org/10.1007/s00231-004-0552-2

[26] Ramya, Dodda, R. Srinivasa Raju, J. Anand Rao, and A. J. Chamkha. "Effects of velocity and thermal wall slip on magnetohydrodynamics (MHD) boundary layer viscous flow and heat transfer of a nanofluid over a non-linearly-stretching sheet: a numerical study." *Propulsion and Power Research* 7, no. 2 (2018): 182-195. https://doi.org/10.1016/j.jppr.2018.04.003

[27] Raza, Jawad. "Thermal radiation and slip effects on magnetohydrodynamic (MHD) stagnation point flow of Casson fluid over a convective stretching sheet." *Propulsion and Power Research* 8, no. 2 (2019): 138-146. https://doi.org/10.1016/j.jppr.2019.01.004

[28] Roşca, Natalia C., and Ioan Pop. "Unsteady boundary layer flow of a nanofluid past a moving surface in an external uniform free stream using Buongiorno's model." *Computers & Fluids* 95 (2014): 49-55. https://doi.org/10.1016/j.compfluid.2014.02.011

[29] Sakiadis, Byron C. "Boundary-layer behavior on continuous solid surfaces: I. Boundary-layer equations for two-dimensional and axisymmetric flow." *AIChE Journal* 7, no. 1 (1961): 26-28. https://doi.org/10.1002/aic.690070108

[30] Soundalgekar, V. M. "Viscous dissipation effects on unsteady free convective flow past an infinite, vertical porous plate with constant suction." *International Journal of Heat and Mass Transfer* 15, no. 6 (1972): 1253-1261. https://doi.org/10.1016/0017-9310(72)90189-5

[31] Thirupathi, Gurrala, Kamatam Govardhan, and Ganji Narender. "Radiative Magnetohydrodynamics Casson Nanofluid Flow and Heat and Mass Transfer past on Nonlinear Stretching Surface." *Beilstein Archives* 2021, no. 1 (2021): 1-22. https://doi.org/10.3762/bxiv.2021.65.v1

[32] Vajravelu, K., and A. Hadjinicolaou. "Heat transfer in a viscous fluid over a stretching sheet with viscous dissipation and internal heat generation." *International Communications in Heat and Mass Transfer* 20, no. 3 (1993): 417-430. https://doi.org/10.1016/0735-1933(93)90026-R

[33] Weidman, P. D., D. G. Kubitschek, and A. M. J. Davis. "The effect of transpiration on self-similar boundary layer flow over moving surfaces." *International Journal of Engineering Science* 44, no. 11-12 (2006): 730-737. https://doi.org/10.1016/j.ijengsci.2006.04.005

[34] Yang, Won Young, Wenwu Cao, Tae-Sang Chung, and John Morris. *Applied numerical methods using MATLAB®*. John Wiley & Sons, 2005. https://doi.org/10.1002/0471705195

[35] Zulkifli, Siti Norfatihah, Norhafizah Md Sarif, and Mohd Zuki Salleh. "Numerical solution of boundary layer flow over a moving plate in a nanofluid with viscous dissipation: A revised model." *Journal of Advanced Research in Fluid Mechanics and Thermal Sciences* 56, no. 2 (2019): 287-295.